arXiv:1605.05161v2 [cond-mat.stat-mech] 16 Jun 2016

Self-Organized Bistability Associated with First-Order Phase Transitions

Serena di Santo,[1,2,3] Raffaella Burioni,[2,3] Alessandro Vezzani,[4,2] and Miguel A. Muñoz[1]

[1] *Departamento de Electromagnetismo y Física de la Materia e Instituto Carlos I de Física Teórica y Computacional. Universidad de Granada. E-18071, Granada, Spain*
[2] *Dipartimento di Fisica e Scienza della Terra, Università di Parma, via G.P. Usberti, 7/A - 43124, Parma, Italy*
[3] *INFN, Gruppo Collegato di Parma, via G.P. Usberti, 7/A - 43124, Parma, Italy*
[4] *IMEM-CNR, Parco Area delle Scienze 37/A - 43124 Parma, Italy*

Self-organized criticality elucidates the conditions under which physical and biological systems tune themselves to the edge of a second-order phase transition, with scale invariance. Motivated by the empirical observation of bimodal distributions of activity in neuroscience and other fields, we propose and analyze a theory for the self-organization to the point of phase-coexistence in systems exhibiting a first-order phase transition. It explains the emergence of regular avalanches with attributes of scale-invariance which coexist with huge anomalous ones, with realizations in many fields.

Multistability –understood as the existence of diverse stationary states under a fixed set of conditions– is ubiquitous in physics and in biology [1–3]. Bistable switches are a common theme in the regulation of cellular processes such as cycles, differentiation and apoptosis [4] and, often, genes are expressed in huge episodic bursts interspersed with periods of quiescence [5]. The cerebral cortex exhibits bistability during deep sleep, with an alternation between high or low levels of neural activity [6–8]. Real neural networks, both *in vitro* and *in vivo* have been reported to exhibit power-law distributed avalanches of activity –interpreted to be a sign of underlying criticality– [9]; however, when inhibitory mechanisms are repressed or under epileptic conditions [10], very large events (beyond the expectations of criticality) appear, and size-distributions become bimodal, suggesting some kind of underlying bistability.

Here we are interested in spatially extended noisy systems –such as the whole cortex or gene-expression patterns across tissues– for which a statistical mechanics framework is most appropriate. In this context, bistability is tantamount to the existence of a first-order phase transition at which two phases coexist [2]. A cornerstone result of equilibrium thermodynamics, the *Gibbs' phase rule*, establishes that two phases can coexist only at a single transition point of a one-dimensional parameter space [2] (see however, [11]). Thus, if biological systems operate in regimes of bistability, there should exist mechanisms by which they self-tune to the edge of a first-order phase transition. This idea resembles the rationale behind self-organized criticality (SOC) [12–16], which explains why critical-like phenomena are ubiquitous despite the fact that second-order phase transitions, with their associated criticality, power-laws and scaling, occur only at singular points of phase spaces. SOC toymodels, such as sandpiles [12, 17, 18]), illustrate how self-tuning to criticality may occur (see below). Theoretical progress [16, 19–21] allowed for a rationalization of how SOC works, by relating it to a standard second-order phase transition [2, 22].

The purpose of the present Letter is to formulate a general theory of *self-organized bistability* (SOB) or self-organized phase coexistence by extending ideas of self-organization to bistable systems. To this end, we recapitulate existing models and theory of SOC and modify them to describe systems exhibiting a first-order phase transition.

Standard vs. "facilitated" sandpiles". We start focusing on an archetypical SOC model: the stochastic Manna sandpile [17]. We analyze both, its standard version and a modified one. Sandgrains (i.e. discrete tokens of stress or "energy") are progressively injected at random sites of a spatially extended system one at each time step (slow timescale). Whenever a certain local threshold (e.g. $z = 3$) is exceeded, the corresponding site becomes unstable and all its sandgrains are redistributed randomly (as opposed to deterministically in the original sandpile [23]) among its nearest neighbors, possibly generating a cascade of activity or "avalanche". The dynamics is conserving, except at the boundaries where sandgrains are "dissipated" [24]. When avalanches stop the addition of grains is resumed, implementing a perfect separation of timescales. Iteration of this slow-driving/dissipation mechanism leads to a steady state in which avalanche sizes and durations are distributed as $P(s) \sim s^{-\tau}$ and $P(t) \sim t^{-\tau_t}$ up to a system-size dependent cutoff [13, 14, 16, 25–27].

Early experimental attempts aimed at observing scale-invariant (SOC) avalanches in real sandpiles did not find the expected power-law distributions. Instead, they found anomalously large quasi-periodic avalanches, that exceeded the expectations for large events in SOC (see, e.g. Fig.4 in [28]). The reason for this is that real sandgrains have a tendency to keep on moving once they start doing so, dragging other grains, and *facilitating* the emergence of huge avalanches. To mimic this effect in a highly-stylized way, we consider the Manna sandpile and modify it with a facilitation mechanism. In particular, we let sites that receive grains simultaneously from more than one neighbor (e.g. from 2) to temporarily (one timestep) decrease their instability threshold (e.g. to $z = 1$). This

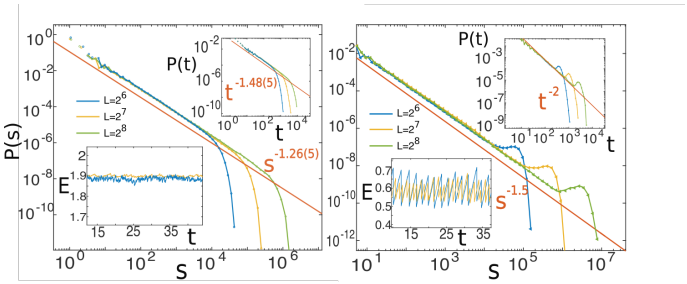


FIG. 1. Avalanche size distributions for the (LEFT) standard 2-dimensional Manna sandpile model and the (RIGHT) facilitated sandpile model (time distributions for the 2 cases are shown in the upper insets). Observe the difference in the avalanche exponents, corresponding to the so-called Manna class in the standard (SOC) case ($\tau \approx 1.26$, $\tau_t \approx 1.48$) versus ($\tau \approx 3/2$, $\tau_t \approx 2$) for the facilitated sandpile. In the facilitated case there are bumps of anomalously large avalanches or "kings" [29]. The lower insets illustrates that"energy" time series are much more sawtooth-like in the facilitated than in the SOC case owing to the existence of "kings".

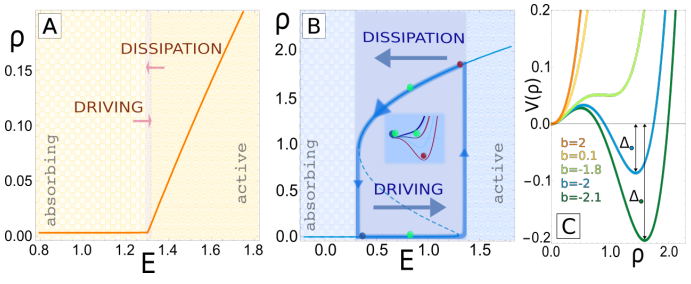


FIG. 2. Sketch of how –within mean-field theory– the self-organization mechanism (alternating driving and dissipation at infinitely separated timescales) tunes to (A) the critical point of a second-order phase transition (SOC) or (B) to the hysteretic loop of a first-order one. In inset in (B) sketches the shape of the potential V and the position of the minima (color code as in the dots of the main plot) as E is changed. (C) Potential, $V(\rho)$ for different values of b, both positive (one minimum) and negative (two minima). For $b < 0$, the potential depth at the active minima, Δ, grows with $|b|$. Parameters: $a = -1.3$, $\omega = c = 1$.

type of cooperative activation is expected to generate discontinuous transitions [22]. Steady-state avalanche-size distributions $P(s)$ for this facilitated sandpile are plotted in Fig.1 for different linear system sizes, L. Two facts are in blatant contrast with usual sandpile results (also portrayed in Fig.1): **(i)** the distributions are *bimodal* and consist of two different types of avalanches: "regular ones" and huge avalanches or "kings" [29] – corresponding to the bumps in the distributions– which reverberate through the whole system, and **(ii)** regular avalanches are (nearly) power-law distributed, but with an exponent $\tau \approx 1.5$ significantly different from the value $\tau = 1.26(5)$ of standard sandpiles [30], [31]. The relative abundance of regular and king avalanches can be altered by changing model details. In any case, the resulting bimodal distributions stem from the self-organization to a state of bistability, as will shall show by putting these findings onto a much general framework: the theory of SOB.

SOC vs SOB: mean-field picture– The key idea to elucidate how SOC works consists in "regularizing" sandpiles by switching off slow driving and boundary dissipation. In this way, the total amount of sand (that we call "energy", E) becomes a conserved quantity that can be used as a control parameter [16, 19, 20]. In the "*fixed-energy ensemble*" the system can be either in an *active phase* (with perpetual activity) for large values of E, or in an absorbing phase (where dynamics ceases) for sufficiently small values of E [22]. Separating these two phases, there is a critical point, E_c, at which a standard second-order phase transition occurs. In this setting, SOC is understood as a dynamical mechanism which, by exploiting slow driving and energy dissipation at infinitely separated timescales, self-tunes the system to E_c [12, 14, 15, 27]). To illustrate these ideas, let us recall how do they operate in the simplest possible mean-field framework [32]. For this, we consider, the minimal form $\dot{\rho}(t) = a\rho - b\rho^2$ for a (mean-field) continuous phase transition separating an absorbing phase with vanishing activity $\rho = 0$ (for $a < 0$) from an active one $\rho = a/b \neq 0$ (for $a > 0$); $b > 0$ is a constant (see Fig.2). This equation is now coupled to an additional conserved "energy" variable E fostering the creation of further activity, $\dot{\rho}(t) = (a+\omega E)\rho - b\rho^2$, where $\omega > 0$ is a constant. For sandpiles, E represents the total density of sandgrains while ρ is the density of sites above threshold. In the fixed-energy variant, E is a conserved quantity, and the critical point lies at $E_c = -a/\omega$. Instead, in the SOC version E is a dynamical variable, as an arbitrarily small driving rate, h, and activity-dependent energy dissipation, ϵ are switched on: $\dot{E} = h - \epsilon\rho$. In the double limit, $h, \epsilon \to 0$ with $h/\epsilon \to 0$ the steady-state solution is $E = E_c$, i.e. the system self-organizes to criticality.

To construct a mean-field theory of SOB, one needs to replace the model showing a continuous transition, by its counterpart for a discontinuous one: $\dot{\rho}(t) = a\rho - b\rho^2 - c\rho^3$, with $b < 0$ and $c > 0$ (the r.h.s. derives from the potential $V(\rho)$ shown in Fig.2, and can be obtained from the continuous-transition case by assuming an additional facilitation effect). Indeed, to implement a positive feedback (facilitation) one needs to increase the a, in the presence of activity, as $a \to a + \alpha\rho$, where α is some constant shifting $-b$ toward larger values $b \to -b + \alpha$. Also, an additional cubic term is included to avoid $\rho \to \infty$. For the above equation, there is a regime of bistability for the active and absorbing states, the domains of attraction of which are separated by the *spinodal* line (dashed line in Fig.2B). Coupling, as in SOC, this dynamics to that of an energy field, $\dot{E} = h - \epsilon\rho$, the system follows a limit cycle (the hysteretic loop in Fig.2): a departure

from the absorbing/active state is observed only when local stability is lost (ending points of the spinodal line). Therefore, within the mean-field approximation, a self-organizing mechanism identical to that of SOC leads to cyclic bursts of activity –i.e. a sort of phase alternance [33]– rather than to a unique point.

SOC vs SOB: beyond mean-field– To investigate how this simple mean-field picture changes in spatially-extended noisy systems, we first recap the stochastic theory of SOC and, then, extend it to first-order transitions. The phase transition of SOC systems, in their fixed-energy counterpart, is described, by the following set of Langevin equations incorporating spatial coupling (diffusion) and noise in a parsimonious way:

$$\begin{aligned} \partial_t \rho(\vec{x},t) &= [a+\omega E(\vec{x},t)]\rho - b\rho^2 + D\nabla^2\rho + \sigma\eta(\vec{x},t) \\ \partial_t E(\vec{x},t) &= D\nabla^2\rho(\vec{x},t) \end{aligned} \tag{1}$$

where $\rho(\vec{x},t)$ and $E(\vec{x},t)$ are fields (some dependencies on $(\vec{x},t)$ have been omitted), $b>0$, D and σ are the diffusion and noise constants, respectively, and $\eta(\vec{x},t)$ is a zero-mean multiplicative Gaussian noise with $\langle\eta(\vec{x},t)\eta(\vec{x'},t)\rangle = \rho(\vec{x},t)\delta(\vec{x}-\vec{x'})\delta(t-t')$ imposing the absorbing state condition. Eq.(1) was proposed on phenomenological grounds [19, 20] (see also [34]) but it can be rigorously derived from microscopic rules (using a coherent-state path-integral representation [35]) [36].

The fixed-energy theory described by Eq.(1) exhibits a continuous phase transition at $\bar{E}_c$ (where $\bar{E}$ is the spatially averaged energy). More remarkably, switching on slow-driving and boundary dissipation in Eq.(1) [37] it self-organizes to $\bar{E}^* = \bar{E}_c$. The width of the spatially-averaged energy distribution $P(\bar{E})$ in the SOC ensemble around $\bar{E}_c$ becomes progressively smaller as system size is enlarged, ensuring that in the thermodynamic limit the system self-organizes exactly to its critical point [38]. This Langevin approach has allowed for establishing a connection between SOC and standard non-equilibrium phase transitions [15, 16, 19, 20], allowing for further computational and theoretical [39, 40] understanding.

In full analogy with the mean-field case, we propose the following equations for discontinuous transitions:

$$\begin{aligned} \partial_t \rho(\vec{x},t) &= [a+\omega E(\vec{x},t)]\rho - b\rho^2 - c\rho^3 + D\nabla^2\rho + \sigma\eta(\vec{x},t) \\ \partial_t E(\vec{x},t) &= D\nabla^2\rho(\vec{x},t), \end{aligned} \tag{2}$$

with $b<0$ and $c>0$. In what follows, we vary b (keeping other parameters fixed) to explore whether diverse regimes emerge. Direct numerical integration of Eq.(2) can be performed in a very efficient way using the split-step integration scheme of [39]. Simulations are started by either low or high densities to enable the system to reach different homogeneous steady states, which are separated by a spinodal line. Results, summarized in Fig.3, confirm that both the size of the jump and the bistability region shrink upon reducing $|b|$ and that they shrink significantly with respect to their mean-field values (Fig.2).

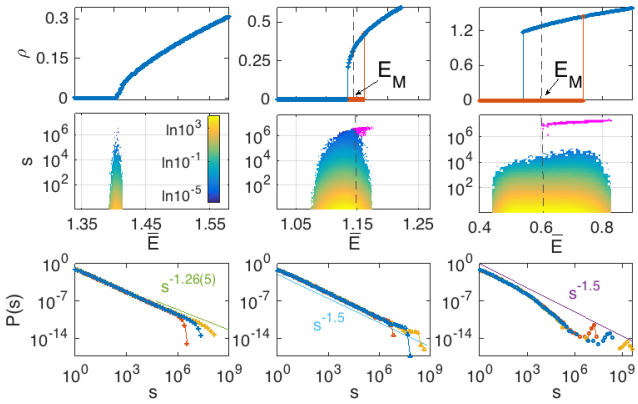


FIG. 3. The three rows show: (Upper) steady state density ρ as a function of E in the fixed-E ensemble, (Central) color-temperature plot of the conditional size distributions $P(s|\bar{E})$ as a function of E; king avalanches plotted with a distinct color (magenta), and (Lower) $P(s)$ for different system sizes; for large $|b|$, king avalanches coexist with smaller ones. The three columns show three different values of $b<0$, ($b=-0.1$, $b=-1$ and $b=-2$, respectively) representatives of different regimes. System size in the first two rows is $L^2=2^{12}$, and $L^2=2^{12},2^{14},2^{16}$ in the bottom one. Parameter values: $a=-1.3$, $\omega=c=D=\sigma=1$.

Remarkably, for small values, e.g. $b=-0.1$, the transition becomes continuous, even if the mean-field approximation predicts a discontinuous one. As discussed in [41], fluctuation effects typically soften the discontinuity, shrink bistability regions, and can even alter the order of the phase transition, leading to noise-induced criticality. For values of $|b|$ larger than a certain (unspecified) tricritical value $|b_T|$ the transition remains discontinuous [42]. We have also verified that there exists a point of true phase coexistence within the bistability regime, i.e. a *Maxwell point* (defined as the value of $\bar{E}$, E_M, at which a flat interface separating two halves of the system, one in each phase, does not move on average, while, for $\bar{E}<E_M$ (resp. $\bar{E}>E_M$) the absorbing (active) phase invades the other one; see dashed lines in Fig.3). Moreover, the observed metastability region shrinks upon enlarging system size.

Having characterized the fixed-energy ensemble, we now let the system self-organize by switching on slow driving and boundary dissipation as in SOC, and allow the system to reach its steady state. As illustrated in Fig.3, we observe different scenarios depending of the value of $|b|$: *(i) Noise-induced critical regime*– For sufficiently small values of $|b|$ (such as $b=-0.1$) the transition becomes continuous and the phenomenology is as in SOC (scale-invariant avalanches with $\tau\approx 1.26$ and $\tau_t\approx 1.48$). *(ii) King-avalanche dominated regime*– In the opposite limit of large values of $|b|$ (e.g. $b=-2$), we observe large peaks in $P(s)$ and $P(t)$ for large events or "kings", coexisting with smaller (regular) avalanches

which are exponentially truncated above a characteristic cutoff time/size, and are responsible for large energy-dissipation events. *(iii) Hybrid regime*– For intermediate values of $|b|$ (e.g. $b = -1.0$), one has a situation similar to that of the facilitated sandpile (Fig.1), in which power-law distributed regular avalanches (with $\tau \approx 3/2$ and $\tau_t \approx 2$) coexist with kings. In cases *(ii)* and *(iii)*, $E(t)$ exhibits characteristic sawtooh-like profiles (as the facilitated sandpile of Fig.1) which –as revealed by the presence of a clear peak in their power spectra (not shown)– are quasi-periodic, i.e. E cycles between high and low values (the larger $|b|$ the larger the excursions). Indeed, Fig.3 (central) shows the conditional distribution $P(s|\bar{E})$, illustrating that avalanches can be triggered at diverse values of $\bar{E}$. However, even if for any finite system, SOB leads to excursions all through the bistability region, we have verified that such regions (and excursions) shrink upon enlarging system size; thus, in the thermodynamic limit, $\bar{E}$ self-tunes in SOB systems to a unique point of phase coexistence –the Maxwell point– much as in SOC [21] and unlike the mean-field picture.

Let us now describe the properties of regular and king avalanches. For regular ones, recall that right at the Maxwell point $\bar{E} = E_M$ both phases are equally stable, and thus the dynamics is as in the so-called compact directed percolation [43] or voter model, in which a stable phase tries to invade an equally stable one, giving rise to a complex dynamics at the boundaries separating both. This type of dynamics is well-known to lead to $\tau = 3/2$ and $\tau_t = 2$ in two (or larger) dimensions [30, 43, 44], [45], so that –as $\bar{E}$ wanders around E_M– one could anticipate that $P(s) \sim s^{-3/2}$ for regular avalanches, with some cut-off that depends on $|b|$ (see below).

As illustrated in Fig.3, king avalanches (magenta color) can be triggered whenever $\bar{E}$ is above the Maxwell point of the fixed-energy diagram (Fig.3), i.e. $\bar{E} \geq E_M$ (and not only when $\bar{E}$ reaches the limit of instability of the absorbing state, as happens in the mean-field picture). The reason for this lies in the existence of a nucleation process [1] as we describe now. Imagine that, after driving the system, a large fluctuation creates a large droplet of activity –of linear size/radius R– in an otherwise absorbing configuration. To investigate the fate of such a droplet in a simple though approximate way, we switch off noise by fixing $\sigma = 0$ in Eq.(2). In this deterministic approximation, one can safely define a free energy which has two additive contributions: one for the space integral of the potential $V(\rho)$ (shown in Fig.2C), and a surface tension term proportional to $D \int d\vec{x} (\nabla\rho)^2$. When $\bar{E} > E_M$, the potential at the active steady state ($\rho > 0$) is negative ($\Delta < 0$) and thus, deeper than that at 0 (Fig.2C). Thus, the creation of an active droplet leads to a competition between the gain of bulk free energy and the penalty associated with the formation of an interface between the active and absorbing states. Equating these two trends, one obtains a critical radius $R_c \approx 2D/\Delta$ above which the bulk contribution dominates and the droplet expands ballistically and compactly through the whole system [1], giving rise to a "king avalanche". This heuristic argument does not strictly apply in the presence of (multiplicative) noise for which a free energy cannot even be defined. However, recent analytical work has shown that the most probable path to jump from active to inactive states in this type of bistable noisy systems involves the creation of a critical droplet that then expands ballistically through the system [46], putting under more solid grounds our heuristic approach. Finally, observe that the larger $|b|$ the smaller R_c, and the stronger the cut-off for regular avalanches.

To visualize these effects, we have kept track of different avalanches –both regular and kings– and computed their averaged shape [47]; this is close to a semicircle for regular avalanches, as correspond to random-walk like processes [47], while kings, after a transient time, have a radically different triangular shape (with linear growth stemming from ballistic expansion, followed by ballistic extinction stemming from large energy dissipation) [48].

In summary, we have defined the concept of "self-organized bistability" (SOB) by extending well-known ideas of self-organization to critical points to systems exhibiting bistability and phase coexistence and provided an explanation for the emergence of bimodal distributions –combining aspects of scale invariance and bistability– as often observed in biological problems. Our goal here is not that of analyzing a specific example of a real system exhibiting SOB –of which we believe there are plenty of instances– but rather to characterize the general mechanism, much as done in SOC. The most promising specific example to be pursued is that provided by real neural networks (for which synaptic resources play the role of E and neural activity that of ρ), in which avalanches appear to be distributed with exponents $\tau \approx 3/2$ and $\tau_t \approx 2$ [9]. These values –at odds with the expectations of SOC in either 2 or 3-dimensional systems– are usually justified by making assumptions about the architecture of the underlying network of connections, a hypothesis which is not always obvious. Furthermore, anomalously large (king) events, inconsistent with the predictions from criticality, appear when inhibitory mechanisms are repressed or under epileptic conditions [10] and a non-trivial temporal organization of neural avalanches [49] has been reported to exist. Thus, we suggest that it should be carefully scrutinized under which circumstances cortical networks (which are known to have facilitation mechanisms) are not self-organized to a critical point (SOC) –as usually considered– but to a region of bistability (SOB) with its concomitant mean-field like avalanche exponents, the natural possibility of king avalanches, and a non-trivial temporal organization. In future work, we shall extend our theory in a number of ways, including self-organization in the absence of conservation laws and/or of infinitely separated time-scales, as

well as allowing for global rather than point-like driving; these extensions will hopefully allow for a more direct connection with biological systems.

We are grateful to the Spanish-MINECO for financial support (under grant FIS2013-43201-P; FEDER funds) and to J.A. Bonachela, J. Hidalgo, and P. Moretti for extremely useful comments.

[1] K. Binder, Rep. Prog. Phys **50**, 783 (1987).
[2] J. Binney, N. Dowrick, A. Fisher, and M. Newman, *The Theory of Critical Phenomena* (Oxford Univ. Press, Oxford, 1993).
[3] A. Pigorini *et al.*, Neuroimage **112**, 105 (2015).
[4] D. Angeli, J. E. Ferrell, and E. D. Sontag, Proc. Nat. Acad. of Sci. **101**, 1822 (2004).
[5] S. Tyagi, Mol. Syst. Biol. **11**, 805 (2015).
[6] D. Holcman and M. Tsodyks, PLoS Comp Biol **2**, e23 (2006).
[7] J. F. Mejias, H. J. Kappen, and J. J. Torres, PLoS One **5**, e13651 (2010).
[8] J. Hidalgo, L. F. Seoane, J. M. Cortés, and M. A. Munoz, PloS one **7**, e40710 (2012).
[9] J. M. Beggs and D. Plenz, J. of Neurosci. **23**, 11167 (2003).
[10] L. De Arcangelis, Eur. Phys. J. Spec.Top. **205**, 243 (2012).
[11] F. de Los Santos, M. T. da Gama, and M. Muñoz, Phys. Rev. E **67**, 021607 (2003).
[12] P. Bak, C. Tang, and K. Wiesenfeld, Phys. Rev. Lett. **59**, 381 (1987).
[13] P. Bak, *How nature works: the science of self-organized criticality* (Copernicus, New York, 1996).
[14] H. J. Jensen, *Self-organized criticality: emergent complex behavior in physical and biological systems* (Cambridge university press, Cambridge, 1998).
[15] G. Pruessner, *Self-organised criticality* (Cambridge Univ. Press, Cambridge, 2012).
[16] R. Dickman, M. Muñoz, A. Vespignani, and S. Zapperi, Braz. J. Phys. (2000).
[17] S. S. Manna, J. Phys. A: Math. Gen. **24**, L363 (1991).
[18] K. Christensen *et al.*, Phys. Rev. Lett. **77**, 107 (1996).
[19] A. Vespignani, R. Dickman, M. A. Muñoz, and S. Zapperi, Phys. Rev. E **62**, 4564 (2000).
[20] A. Vespignani, R. Dickman, M. Muñoz, and S. Zapperi, Phys. Rev. Lett. **81**, 5676 (1998).
[21] J. A. Bonachela and M. A. Muñoz, J. Stat. Mech. P09009 (2009).
[22] H. Hinrichsen, Adv. Phys. **49**, 815 (2000).
[23] The deterministic sandpile model [12] has additional "conservation laws" being thus much harder to analyze.
[24] For SOC mechanisms in non-conserving systems see [21] and refs. therein.
[25] K. Christensen and N. Moloney, *Complexity and criticality* (Imperial College Press, London, 2005).
[26] D. Dhar, Physica A **369**, 29 (2006).
[27] G. Grinstein, *Scale invariance, interfaces, and non-equilibrium dynamics* (Springer, Berlin, 1995), p. 261.
[28] N. Yoshioka, Earth Planets Space **55**, 283 (2003).
[29] D. Sornette and G. Ouillon, Eur. Phys. J. Spec.Top. **205**, 1 (2012).
[30] M. Muñoz, R. Dickman, A. Vespignani, and S. Zapperi, Phys. Rev. E **59**, 6175 (1999).
[31] See Supplemental material at [] for a movie showing the alternance of both types of avalanches.
[32] S. Zapperi, K. B. Lauritsen, and H. E. Stanley, Phys. Rev. Lett. **75**, 4071 (1995).
[33] This switching is not to be confused with stochastic resonance [50] which is a noise induced phenomenon.
[34] M. Paczuski, S. Maslov, and P. Bak, EPL (Europhysics Letters) **27**, 97 (1994).
[35] K. J. Wiese, arXiv preprint arXiv:1501.06514 (2015).
[36] Observe that the $E(\vec{x},t)$ field is a sort of dynamically-generated disorder, different from the "quenched" disorder appearing in other SOC-like phenomena such as Barkhaussen noise [51].
[37] This can be done in different ways; e.g. increasing both $\rho(\vec{x},t)$ and $E(\vec{x},t)$ at a given point by some amount (0.1) to create a new avalanche when the absorbing state has been reached and allowing for energy dissipation at open boundaries.
[38] See [21], and [52–54] for some lingering controversy.
[39] I. Dornic, H. Chaté, and M. A. Muñoz, Phys. Rev. Lett. **94**, 100601 (2005).
[40] J. A. Bonachela, M. Alava, and M. A. Muñoz, Phys. Rev. E **79**, 050106 (2009).
[41] P. Villa Martín, J. A. Bonachela, S. A. Levin, and M. A. Muñoz, Proc. Nat. Acad. of Sci. **112**, E1828 (2015).
[42] P. Grassberger, J. Stat. Mech. **2006**, P01004 (2006).
[43] J. Essam, J. of Phys. A **22**, 4927 (1989).
[44] O. A. Pinto and M. A. Muñoz, PloS one **6**, e21946 (2011).
[45] With the possibility of logarithmic corrections in two dimensions.
[46] B. Meerson and P. V. Sasorov, Phys. Rev. E **83**, 011129 (2011).
[47] A. Baldassarri, F. Colaiori, and C. Castellano, Phys. Rev. Lett. **90**, 060601 (2003).
[48] See Supplemental material at [...] for an illustrative plot.
[49] F. Lombardi, H. J. Herrmann, D. Plenz, and L. De Arcangelis, Front. Syst. Neurosci. **8**, (2014).
[50] K. Wiesenfeld *et al.*, Nature **373**, 33 (1995).
[51] O. Perković, K. Dahmen, and J. P. Sethna, Physical review letters **75**, 4528 (1995).
[52] A. Fey, L. Levine, and D. B. Wilson, Phys. Rev. Lett. **104**, 145703 (2010).
[53] H.-H. Jo and H.-C. Jeong, Phys. Rev. Lett. **105**, 019601 (2010).
[54] S. S. Poghosyan, V. Poghosyan, V. Priezzhev, and P. Ruelle, Phys. Rev. E **84**, 066119 (2011).